Volume 1 | Number 1 | Jan 2013 | Pages 1–100

PCCP

Physical Chemistry Chemical Physics
www.rsc.org/pccp

ROYAL SOCIETY OF CHEMISTRY

ROYAL SOCIETY OF CHEMISTRY

www.rsc.org/pccp

Insights into Hydrophobic Molecule Release from Polyelectrolyte Multilayer Films Using *In Situ* and *Ex Situ* Techniques

Yongjin Shin [1], Weng Hou Cheung [2], Tracey T.M. Ho [1], Kristen E. Bremmell [2]*, David A. Beattie [1]*

[1] Ian Wark Research Institute, University of South Australia, Mawson Lakes Campus, Mawson Lakes, SA 5095

[2] School of Pharmacy and Medical Sciences, University of South Australia, City East Campus, North Terrace, Adelaide, SA 5000

* Corresponding authors: Kristen.Bremmell@unisa.edu.au; David.Beattie@unisa.edu.au

Abstract

We report on the loading and release of curcumin (a hydrophobic polyphenol with anti-inflammatory and anti-bacterial properties) from polyelectrolyte multilayers composed of poly(diallyldimethylammonium chloride) (PDADMAC) and poly(sodium 4-styrenesulfonate) (PSS). We have used the *in situ* techniques of attenuated total reflectance (ATR) FTIR spectroscopy and quartz crystal microbalance with dissipation monitoring (QCM-D) to study the formation of the PEM and the incorporation of curcumin, providing direct evidence of the incorporation, in terms of molecular vibrations and gravimetric detection. The release of curcumin was followed using *ex situ* measurements of UV-visible spectroscopy of PEM films on quartz plates, in addition to *in situ* ATR FTIR measurements. Release was studied as a function of salt concentration of the release solution (0.001 M NaCl; 1 M NaCl). UV-visible spectroscopy indicated that salt concentration of the release solution had a major impact on release rates, with higher salt giving faster/more extensive release. However, prolonged timescale immersion and monitoring with UV-visible spectroscopy indicated that sample dehydration/rehydration cycling (required to measure UV absorbance) was responsible for the release of curcumin, rather than immersion time. *In situ* measurements of release kinetics with ATR FTIR confirmed that release does not occur spontaneously while the multilayer remains hydrated.

Introduction

The storage and release of small hydrophobic molecules from dispersed colloidal systems, or surface treatments applied to materials, is of fundamental interest in areas as diverse as drug delivery [1-3], wound healing [4], marine biofouling [5], and food processing [6]. One class of molecules of particular interest for such applications is the group of polyphenols [4, 7], carotenoids [6], and other co-called bio-active nutraceuticals. These molecules straddle the boundary between drugs and nutrients, and often have demonstrated clinical effectiveness for a wide range of conditions.

Curcumin [1,7-bis-(4-hydroxy-3-methoxyphenyl)-1,6-heptadiene-2,5-dione], an extract of the turmeric root, is one such lipophilic polyphenol. Curcumin has demonstrated antioxidant, anti-inflammatory, anti-tumorigenic properties, and has found application in cancer therapeutics (see for example [8], [9], [10]). There has been increasing interest in delivery of curcumin to different sites in the body, using delivery vehicles such as emulsions [11], liposomes [12] and polymeric nanoparticles [13] and fibers [4]. There is also interest in the incorporation of curcumin in surface treatments for surface-mediated drug delivery, through the use of polyelectrolyte multilayers (often referred to as PEMS) [1, 14].

PEMs are formed through layer-by-layer self-assembly of polyanionic and polycationic species, and are a drug delivery vehicle that is heavily investigated in biomaterials science [15-19]. As a drug delivery platform, polyelectrolyte multilayers provide a versatile carrier system, with the ability to manipulate aspects such as charge, permeability, functional groups and the hydrophobic/hydrophilic nature of the films, which can impact on the loading and release behaviour of drug molecules. Therefore, understanding loading and release of various molecules within the PEMs is a crucial step in developing these systems for lipophilic molecule delivery.

Kittitheeranun *et al*. [14] have studied the loading of curcumin into multilayer films of poly

(diallydimethylammonium chloride) (PDADMAC) and poly (sodium 4-styrenesulfonate) (PSS). Their stated aim was to consider the potential for curcumin uptake from transdermal patches, presumably of the first generation type [3, 20], which relies on the lipophilic nature of the molecule to aid its passage through the stratum corneum. They found the concentration of loaded curcumin to be proportional to the number of multilayers, and therefore that curcumin diffused into the bulk of the layers and did not just adsorb on the outer layer.

While curcumin is a lipophilic molecule, the driving force for curcumin incorporation in the PEM was reported to be a partitioning mechanism where the PEM was considered the hydrophobic phase and the water/ethanol solvent the hydrophilic phase. They argued that while the polyelectrolytes are charged, when formed into multilayers, the complexes are insoluble and have a hydrophobic component which provides a favorable environment for the lipophilic curcumin. Release of curcumin from these PEMs was not mentioned. However despite the lipophilic nature of curcumin, previous studies have reported the release of curcumin from various polymeric carriers into phosphate buffer solution (PBS) at pH 7 [13, 21].

In this study, curcumin loading and release from PDADMAC/PSS multilayer films was investigated using *ex-situ* UV-VIS and the *in-situ* techniques of quartz crystal microbalance (QCM) with dissipation monitoring [22, 23], and attenuated total reflection (ATR) Fourier transform infrared (FTIR) spectroscopy [24, 25]. By combining both *in situ* and *ex situ* techniques, we have been able to assess the influence of sample dehydration/rehydration (which is required for *ex situ* analysis of the curcumin-loaded PEMS) on release behaviour.

A single solution composition was chosen to load the curcumin, but solutions of varying ionic strength were used to study the release. Swelling and permeability of polyelectrolyte multilayers have been shown to depend on ionic strength both during construction and on completed PEMs [26-28], and thus ionic strength is a natural parameter to vary in our investigation.

4

MATERIALS AND METHODS

Materials

Aqueous solutions of poly(sodium 4-styrenesulfonate) (PSS; molecular weight (MW), ~70,000 Dalton, powder) and poly(diallydimethylammonium chloride) (PDADMAC; molecular weight (MW), ~200 000-350 000 Dalton; 20% solution) were purchased from Sigma-Aldrich. All the solutions for formation of polyelectrolyte multilayers were prepared one day before, stirred overnight at a concentration of 500ppm, and diluted to 50ppm just prior to use. Background electrolyte for formation of the multilayers was 1M NaCl in milli-Q water (resistivity $18\Omega^{-1}$ cm^{-1}).   No pH modification was used for the polymer solutions for PEM formation, with natural pH values of the two solutions being as follows: PDADMAC – pH 6.8; PSS – pH 7.0.   Curcumin (> 98% purity, Aldrich) was prepared as a 0.001 wt. % solution in 90:10 mixtures of water:ethanol (milli-Q; HPLC grade) for the loading of the PEM.   For the unloading process, the pH of unloading solutions was adjusted with high purity NaOH to pH 7 for either 0.001 M NaCl or 1 M NaCl.   Chemical structures of the two polymers and curcumin are given in Figure 1.
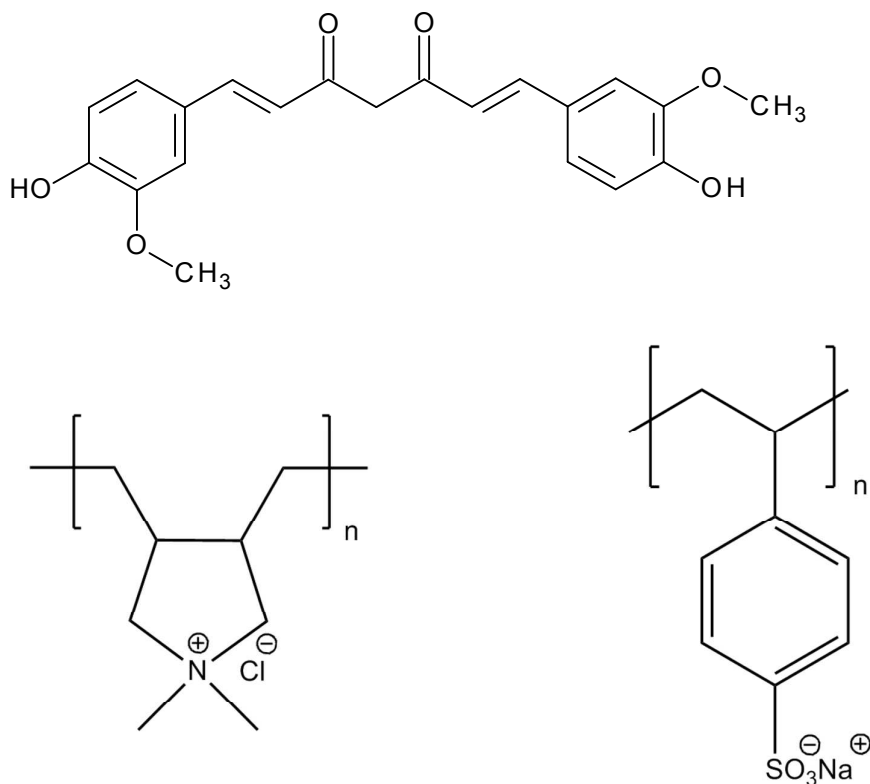
Figure 1: Schematic chemical structures of: top – curcumin; lower left – poly(diallydimethylammonium chloride) (PDADMAC); and lower right – poly(sodium 4-styrenesulfonate) (PSS).

Quartz Crystal Microbalance

The PEM build-up was monitored *in situ* by quartz crystal microbalance with dissipation monitoring (QCM-D, E4, Q-Sense, Sweden). The technique consists of a quartz crystal sandwiched between a pair of electrodes and is excited to oscillate through the application of an AC voltage. The measurements were performed on silica coated AT-cut 5MHz quartz crystals purchased from Q-Sense. Silica-coated sensors were used to provide a negatively charged surface for adsorption of the first polymer layer of the multilayer (polycation PDADMAC).

QCM-D is a echnique that measures the changes in the resonance frequency (Δf) of the oscillating quartz crystal as molecules adsorb onto its surface. The change in dissipation

energy (ΔD) is also measured simultaneously with Δf, providing information on the viscoelasticity of the adsorbed film [29]. The dissipation energy is defined as:

$$D = \frac{E_{lost}}{2\pi E_{stored}}$$

where E_{lost} is the dissipated energy during one oscillation cycle and E_{stored} is the total energy stored in the oscillator.

For a thin and rigid film, the decrease in frequency is related directly to the mass (Δm) of the adsorbed molecules, and can be calculated using the Sauerbrey relation [30]:

$$\Delta m = -\frac{C \cdot \Delta f}{n}$$

where $C = 17.7$ ng Hz^{-1} cm^{-2} for a 5 MHz quartz crystal and $n = 1,3,5,7$ is the overtone number. However, in the case of polyelectrolyte multilayers that are usually soft or viscoelastic in nature due to the hydration water present in the film, the Sauerbrey expression often becomes invalid. Thus, for viscoelastic films, the mass can be deduced using the Voigt model [31], which assumes that the film has a uniform thickness and uniform density.

The QTools software (Q-Sense) and Voigt analysis was used to model the experimental data to obtain viscoelastic properties of the film, such as the shear elastic modulus, μ, and the shear viscosity, η. The changes in frequency and dissipation for the 7th and 9th overtones were fitted. The fixed values used in the model were 0.001 kg/ms for background electrolyte shear viscosity, and 1000 kg/m^3 for the background electrolyte density. The value for the film density was allowed to vary in the fitting between 1050 and 1150 kg/m^3.

The sensors were cleaned by sonication for 30 minutes in 2% Sodium Dodecyl Sulfate (SDS) solution, washed with milli-Q water to remove residual SDS from the surface, dried with N_2 gas, and then cleaned in a plasma cleaner (Harrick Scientific) for 2 minutes. Sensors were placed into flow cells in the instrument, then exposed to flowing solution of 1 M NaCl until the sensor oscillation frequency stabilized. After stabilizing, the formation of the PEM

involved successive exposure to flowing solutions of PDADMAC, NaCl, PSS, NaCl for 10, 5, 10, 5 minutes respectively, until 5 bilayers were formed on the QCM sensor.

ATR FTIR Spectroscopy

A Nicolet 6700 FTIR spectrometer (Thermo-Fisher Scientific) was used for ATR-FTIR formation, incorporation, and release experiments. The instrument was coupled to a Fast-IR single bounce ATR accessory (Harrick Scientific) with a ZnSe ATR crystal and flow cell. The zeta potential of ZnSe at the deposition pH was determined using a ZetaSpin 2.0 instrument (Zetametrix, USA). ZetaSpin uses the well-known principle of streaming potential determination for rotating discs: [32] (i) rotations of the sample induce the radial flow generated near the sample surface; (ii) the flow sweeps charge adjacent to the face of the sample towards the edge of the sample, producing spatially distributed streaming potential [33]. At the solution pH used for the deposition of the first polymer layer (pH 6.8), the ZnSe is negatively charged (approximately -20 mV at 1×10^{-2} M NaCl).

A Masterflex pump (model 77120-70) was used with Tygon tubing (AR-4310 PVC standard pump tube 1.02mm I.D.) for flow of solutions, at a flow rate of approximately 2ml/min. The ATR Crystal was cleaned by polishing with fine silica oxide (OP-U Struers suspension) for 2 min, followed by rinsing with milli-Q water. After the crystal was dried, the crystal was attached to ATR top plate, and placed on the Fast-IR accessory. Flow cell units were sonicated in acetone, methanol, milli-Q water for 15 minutes each.

FTIR spectra were recorded with 1024 scans at a resolution of 4 cm^{-1}. A background spectrum was recorded of the bare clean ATR crystal after 1 hour of dry air purging (40 L/hr). After a further 30 minutes of purging, a sample spectrum of bare crystal was taken to obtain a spectrum of water vapour (for use in post spectral acquisition processing). The flow cell was then attached and a 1 M NaCl solution was introduced into the flow cell, and a sample

spectrum recorded of the electrolyte solution (after 30 min of purging). The same sequence of solution flowing was followed for PEM build-up as was used in the QCM-D formation experiments (PDADMAC, NaCl, PSS, and NaCl was injected for 10, 5, 10, 5 minutes respectively). Spectra were acquired after each bilayer was added to the film.

All spectra were processed to remove the spectrum of the background electrolyte, in addition to spectral interference due to varying purge levels in the instrument (using the spectrum of water vapour). All spectral processing was performed in the OMNIC software package.

UV-visible spectroscopy

For UV-visible absorbance studies, an Evolution 201 UV-Visible Spectrometer (Thermo-Fisher Scientific) was used, which was equipped with a transmission sample holder for analysis of quartz crystal plates (Starna Pty Ltd, 50x25x1.25mm). The wavelength range of the irradiation was 250-700 nm, allowing for acquisition of the full curcumin peak (located approximately 350-550 nm). The quartz plates (like silica) will be negatively charged at the solution pH values used for polymer adsorption [34]. The plates were cleaned using piranha solution (mixture of 3:1 H_2SO_4:30% H_2O_2) for 30 min followed by extensive rinsing in Milli-Q water, N_2 drying, and a 60 s plasma clean (Harrick).

Once cleaned, the quartz plates were dipped into solutions of the various polymers and rinse solutions: PDADMAC, 1M NaCl, PSS, and NaCl solution for 10, 5, 10, 5 minutes respectively. This process was repeated until 5 bilayers were deposited onto the quartz plates. A UV-vis spectrum of a 5-bilayer multilayer was recorded and used as a background for analysis of loading and unloading of curcumin from the multilayer. For the loading process, the substrates were immersed for 12 hours in 0.001% curcumin in a 90:10 water:ethanol solution. The plates were then rinsed in 90:10 water:ethanol for 5 minutes and dried with N_2 gas, and a spectrum recorded. A UV-visible spectrum of a loaded PEM film is

shown in the supporting information, along with pictures of the quartz slides illustrating the distinct yellow colour of the loaded PEM films.

For unloading, the dry plates were immersed in the salt solution for 1 hour, and then rinsed gently with milli-Q water before drying, and spectral acquisition.   The plates were then re-immersed into the unloading solution for another immersion/measurement cycle.

RESULTS

Polyelectrolyte Multilayer Formation and Curcumin Loading

Quartz Crystal Microbalance (QCM-D): Response of the silica-coated QCM sensors (both frequency and dissipation) to exposure to the formation solutions is shown in Figure 2.   The 7th and 9th overtones of the frequency and dissipation response are both plotted.   The different overtones of the frequency response ($\Delta f_n/n$) are almost perfectly overlapped.   The same is not true for the dissipation, with a slight degree of separation for some stages of the polymer film formation; specifically the adsorption of the PDADMAC layer.   The overall increase in frequency is large – indicating the adsorption of a substantial amount of material. However, the dissipation response is low – approximately 2×10^6, a value that indicates that the adsorbed PEM layer is relatively rigid (certainly compared to some studies of single polymer layers [35, 36]).

With such a low value of dissipation, it is relatively safe to use the Sauerbrey expression to determine the mass of polymer material (including hydration water) on the QCM sensor. The QTools software allows one to determine this value to be: 9440 ng / cm^2.   The frequency and dissipation response of the 7th and 9th overtones were used to determine the viscoelastic characteristics of the multilayer using the Voigt model.   The determined parameters were as follows: shear elastic modulus, μ, of 4.7×10^7 Pa; shear viscosity, η, of 0.01 kg/ms; multilayer thickness of 87 nm; multilayer density of 1100 kg / m^3.   These

parameters allow us to further calculate the Voigt mass (per unit area of the sensor) of the adsorbed layer (density multiplied by layer thickness) to yield 9520 ng / cm^2, which is in very good agreement with the Sauerbrey mass (as expected for systems with low dissipation response).

In terms of the build-up of the multilayer, it can be seen that the initial stages of polymer adsorption are fully at equilibrium prior to the rinsing stages and the subsequent exposure to the oppositely charged polymer.   However, as the layer numbers increase, it is clear that 10 minutes of adsorption time does not allow the two polymers to reach their full potential coverage.   In addition, the salt rinse between each polymer addition results in an increasing amount of desorption of loosely bound polymer material (almost no desorption for the first few layers, increasing to approximately 10% desorption for the penultimate polymer layer, i.e. the last PDADMAC adsorption).   In spite of this, it can be seen that the growth of the multilayer is non-linear: the mass increase for each subsequent bilayer is greater than the bilayer before.   A plot of mass versus bilayer number is included in the supporting information, demonstrating the exponential growth of the multilayer with bilayer number.
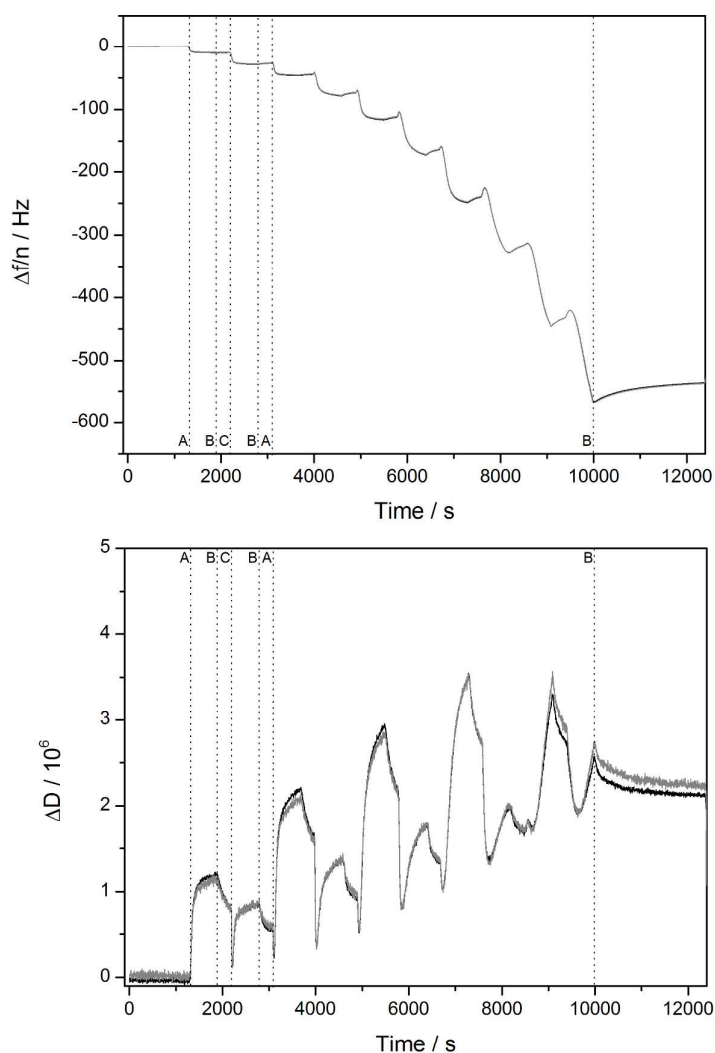
Figure 2: Quartz crystal microbalance (with dissipation monitoring) data for multilayer formation of PDADMAC/PSS on silica-coated QCM sensors. Top: 7th (black) and 9th (grey) overtone frequency change ($\Delta f_n/n$) for the build-up of a 5-bilayer multilayer film. Bottom: 7th (black) and 9th (grey) overtone dissipation change (ΔD) for the build-up of a 5-bilayer multilayer film. A – PDADMAC 50 ppm solution in 1M NaCl; B – rinse solution of 1 M NaCl; C – PSS 50 ppm solution in 1 NaCl. Dotted lines indicate period of first full bilayer formation, and the final rinse.

QCM-D has also been used to monitor the incorporation of curcumin into the polymer multilayer. The formation of the multilayer was performed in the same manner as that described above, with the modification of the solvent rinse stage following multilayer completion. In the case of the incorporation experiment, the rinse solution was a 90:10 water:ethanol solution, to prepare for the flow of the curcumin solution over the multilayer. After a period of approximately 75 minutes (after which time the frequency and dissipation response of the QCM sensor/multilayer assembly had equilibrated) the curcumin solution was introduced. The incorporation was followed until it appeared that the curcumin incorporation had reached a plateau (approximately 2 hours), after which time the multilayer was exposed to another 90:10 water:ethanol solution to determine how much curcumin was irreversibly held within the multilayer.

The QCM data (frequency and dissipation, 7th and 9th overtones) are shown in Figure 3. The multilayer formation section of the plots is very similar to that seen in Figure 2 (QCM analysis for PEM formation in Figure 3 yields the following data: Sauerbrey mass = 9250 ng / cm^2; shear elastic modulus, μ = 5.2 x 10^7 Pa; shear viscosity, η = 0.005 kg/ms; multilayer thickness = 85 nm; multilayer density = 1097 kg / m^3; Voigt mass = 9330 ng / cm^2). At the point of water:ethanol flow into the sensor chamber, the frequency and dissipation response of the sensor can be seen to dramatically alter, as expected based on the significant alteration to the density and viscosity of the solvent. Insertion of the curcumin solution can also be clearly seen, and over the 120 minutes of exposure, the frequency response alters corresponding to a Sauerbrey mass gain of 292 ng / cm^2. Following the rinse of the sensor with blank water:ethanol solution, approximately 155 ng / cm^2 is released from the multilayer. It is likely that continued rinsing with the water:ethanol solution will continue to remove curcumin until the majority is removed from the multilayer. To prevent excessive removal of curcumin from the loaded multilayers prior to use in the unloading experiments

13

(performed with salt solution), only limited rinsing in water:ethanol solution (less than 5 min) was used after incorporation.
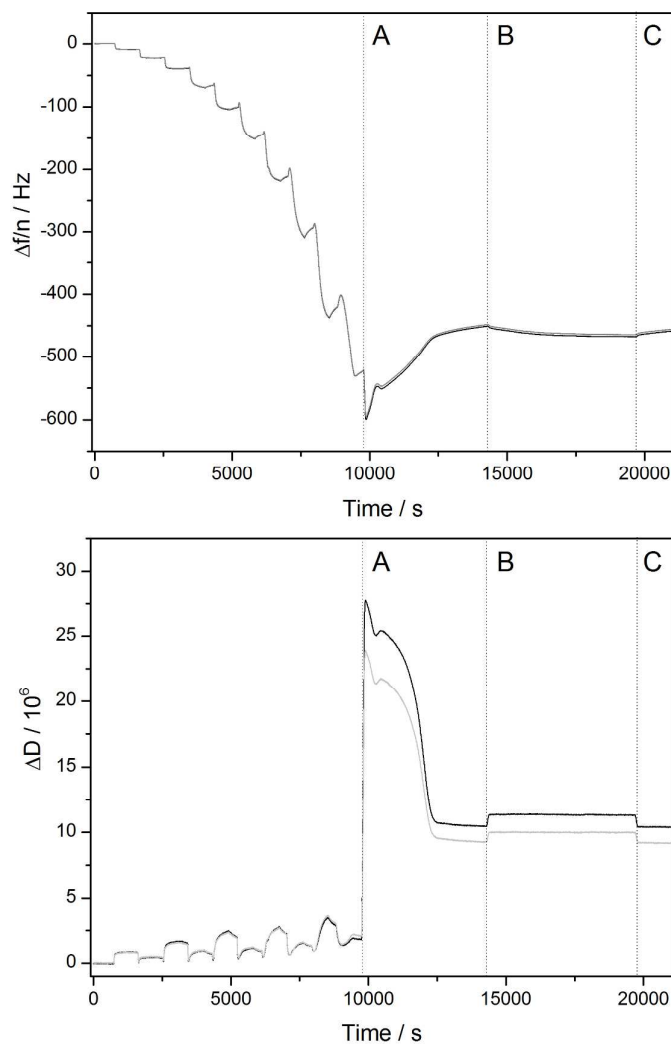
Figure 3: Quartz crystal microbalance (with dissipation monitoring) data for multilayer formation of PDADMAC/PSS on silica-coated quartz sensors and incorporation of curcumin. Top: 7th and 9th overtone frequency change ($\Delta f_n/n$).   Bottom: 7th and 9th overtone dissipation change (ΔD).   Dotted lines indicate: (A) flow of water:ethanol solution; (B) flow of 0.001 wt. % curcumin solution in water:ethanol solution; and (C) flow of water:ethanol solution.

14

ATR FTIR: The same formation and loading conditions described above for QCM experiments were replicated for *in situ* ATR FTIR studies of the multilayer formation. FTIR spectra were acquired after each bilayer was deposited, and the five spectra acquired for the completed multilayer are given in Figure 4 (A: top panel). The spectra are dominated by the vibrations of the sulfonate group of PSS [37-39], with full assignment given in Table 1. The only peak that is exclusive to PDADMAC is the peak for the -CH$_3$ deformation mode at 1473 cm^{-1} [40]. This peak is alongside the –CH$_2$ deformation mode at 1455 cm^{-1} [38] (attributable to both PDADMAC and PSS) and two aromatic ring stretching modes from PSS (1492 cm^{-1} and 1411 cm^{-1}).

As determined from the QCM-D studies, the multilayer is quite thin, even at 5 bilayers thick. The whole assembly is within the first 90 nm of the region that will be probed by the evanescent wave of the FTIR beam (which penetrates up to approx. 1 micron at 1000 cm^{-1}), indicating that the spectral absorbance values will be close to linearly related to the adsorbed mass. With that in mind, inspection of the absorbance values for each bilayer confirms the non-linear growth of the multilayer assembly. The absorbance can be seen to almost double for each bilayer addition. This matches the trend seen with the QCM data, and absorbance versus bilayer number data is plotted along with the QCM mass in the supporting information (and exponential growth confirmed with fitting). It should be noted that if the distance of each bilayer from the surface of the ATR crystal was significant, it would be expected that the absorbance of each subsequent bilayer would be an underestimate of the adsorbed amount relative to the bilayer before.

The incorporation of curcumin was also monitored with ATR FTIR. After the 5-bilayer multilayer was formed on the ATR crystal, the film was exposed briefly (1-2 min) to a 90:10 water:ethanol solution without curcumin, followed by 12 hours of exposure to a flowing solution of curcumin in 90:10 water:ethanol. After immersion, the film was rinsed with

blank 90:10 water:ethanol for 5 minutes, and then a 1M NaCl salt solution was flowed into the ATR flow cell for 5 minutes. Spectra were recorded immediately before the first exposure to a 90:10 water:ethanol solution, and immediately after the 1M NaCl salt solution was re-introduced following incorporation of the curcumin. The PEM pre-loaded spectrum, the PEM loaded spectrum, and the result of spectral subtraction (loaded minus preloaded) are all shown in Figure 4 (B: bottom panel).

Upon comparing the preloaded spectrum with the loaded spectrum, it is clear that incorporation of the curcumin has resulted in the appearance of a number of new spectral peaks. The positions and assignment [41] of these peaks are given in Table 1. The most prominent peak is the aromatic C=C stretching mode at 1514 cm^{-1}, followed by the 1290 cm^{-1} C-O-C stretch. These peaks are more easily seen in the spectral subtraction in Figure 6. These two spectral peaks are visible even without the subtraction, which should allow unambiguous detection of curcumin release from the multilayer.
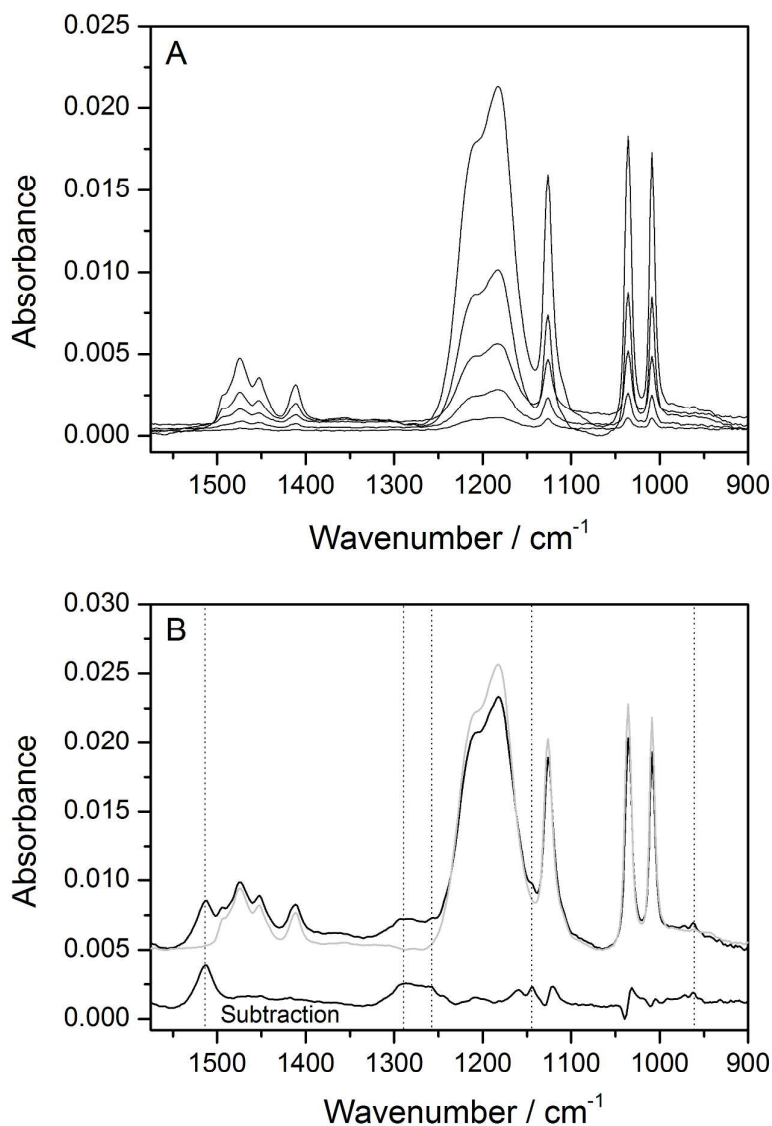
Figure 4: A. ATR FTIR spectra of successive bilayers of a 5-bilayer polyelectrolyte multilayer of PDADMAC and PSS, formed from solutions of 50 ppm in 1 M NaCl electrolyte. B. ATR FTIR spectra of PDADMAC/PSS 5-bilayer multilayers before (grey line) and after loading (upper black line) with curcumin from a 0.001% (by weight) solution in 90:10 water:ethanol. Also shown is the resulting spectral subtraction (lower black line), which highlights the additional spectral peaks that are present after curcumin incorporation. Peak assignments are given in Table 1.

Table 1: Peak positions and assignments for the 5-bilayer polyelectrolyte multilayer (PEM) of PDADMAC and PSS, formed from solutions of 50 ppm in 1 M NaCl electrolyte, and for curcumin loaded into a 5-bilayer PEM.

Peak position / cm^{-1}	Assignment [37-40, 42,41]	Component
1009	Aromatic ring breathing mode	PSS
1036	-SO$_2$- deformation	PSS
1126	-SO$_2$- symmetric stretch	PSS
1182	-SO$_2$- asymmetric stretch	PSS
1208	-SO$_2$- asymmetric stretch	PSS
1411	Aromatic semi-circle stretch	PSS
1452	-CH$_2$ deformation	PSS and PDADMAC
1473	-CH$_3$ deformation	PDADMAC
1492	Aromatic semi-circle stretch	PSS
962	C-H deformation	Curcumin
1144	C-O-H alcohol	Curcumin
1257	-	Curcumin
1290	C-O-C stretch	Curcumin
1514	Aromatic C=C stretch	Curcumin

Curcumin Release

UV Visible Spectroscopy: To probe the kinetics of release, dried PEM-coated/curcumin-incorporated quartz plates were immersed in release solutions (salt solutions of either 1 M NaCl or 0.001 M NaCl at pH 7) for an hour, removed, rinsed, dried, and then placed into the UV-Visible spectrometer to record the decrease in intensity of the curcumin absorbance at 440 nm.   The plates were then re-immersed in the release solution, and the process repeated for five more iterations.   An example of the sequence of spectra thus acquired is given in Figure 7, for release into 0.001M NaCl solution.   The spectral peak of curcumin is at approx. 440 nm, which is slightly altered in position and band shape from that of curcumin in water:ethanol solution [14], due to interaction with the PEM (such as potential π-π interactions between the molecule and the aromatic ring on the PSS.   The peak can be seen to decrease in intensity with each successive 1 hour immersion into the release solution.   The release is quantified in terms of normalized integrated absorbance for the entire peak in the lower plot in Figure 5.   Also given in the lower plot is the same data obtained for the analogous experiment for the 1 M NaCl release solution.   It can be seen that salt concentration of the release solution has a major impact on the release process, with the higher salt solution causing a much greater release of the curcumin from the polymer multilayer.
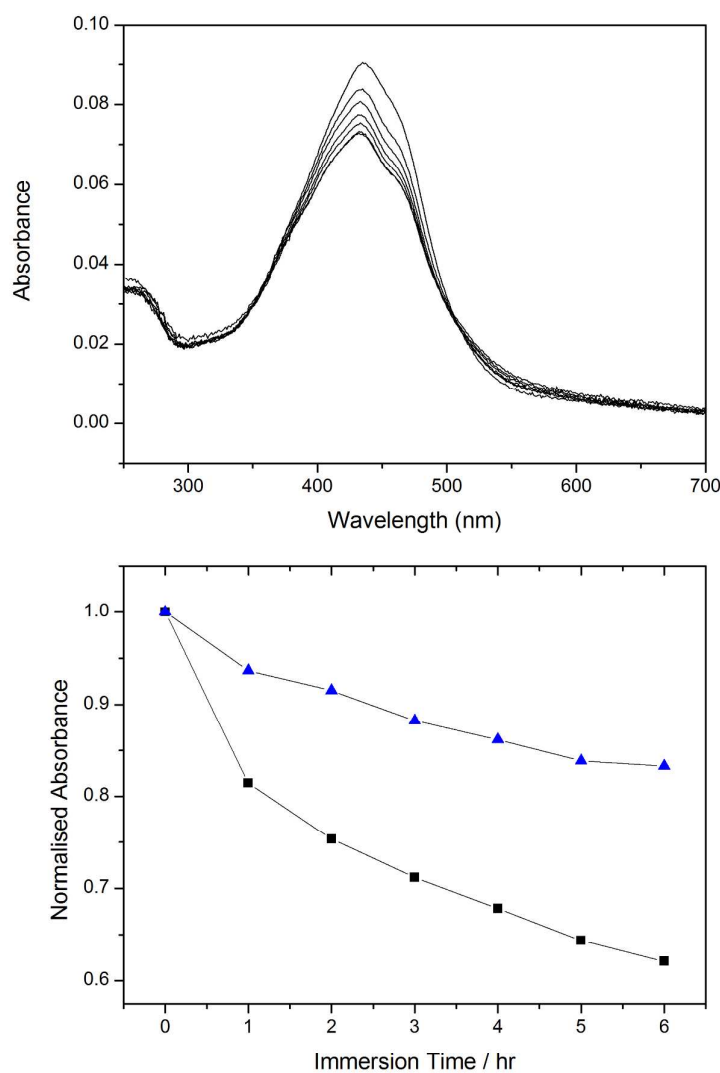
Figure 5: Unloading data, both UV Vis spectra (top) and normalized peak absorbance (bottom), for the release of curcumin from a 5-bilayer PEM of PDADMAC:PSS. The UV Vis spectra are for release into 0.001M NaCl solution. The normalized absorbance data are for both 0.001M NaCl and 1 M NaCl. Filled triangles: 0.001M NaCl release solution. Filled squares: 1M NaCl release solution.

To determine what percentage of curcumin can be released from the multilayer, a much longer immersion time (15 hours) was included in the methodology, after which more regular immersions (every 2 hours) were re-instigated. It was expected that we would be approaching the limiting release value, based on the relatively rapid release observed in Figure 5. The data from this second UV visible experiment is shown in Figure 6. The same trend was observed for the salt concentration variance of the release solution, with the higher salt concentration resulting in greater release (in addition, an additional dataset with an intermediate salt concentration of 0.1 M NaCl was collected for this experiment – see supporting information – which confirms the salt dependence of the release). However, the expected dramatic drop in curcumin content of the multilayers for the 15 hour immersion was not seen. The drop in curcumin content was just marginally more than would have been expected for another 1 hour immersion after the initial 7 individual hourly immersions. Furthermore, the rate of release increased after the shorter immersions were re-instigated. This was entirely unexpected and raises significant questions about the mechanism of release of the curcumin. It is possible that immersion time is not the major determinant in the release of the curcumin.

One potential explanation for the observed data is that release is caused by the rehydration of the polymer multilayer following the drying process (which is required for measurement of the UV Vis absorbance). In this case, the release kinetics would depend on the immersion cycle number, rather than the immersion time. The same UV Vis release data is plotted as a function of immersion cycle, and this is shown in the lower plot in Figure 6. It can be seen that the release curve is much more as expected, with only a minor discontinuity for the cycle immediately following the long time immersion.
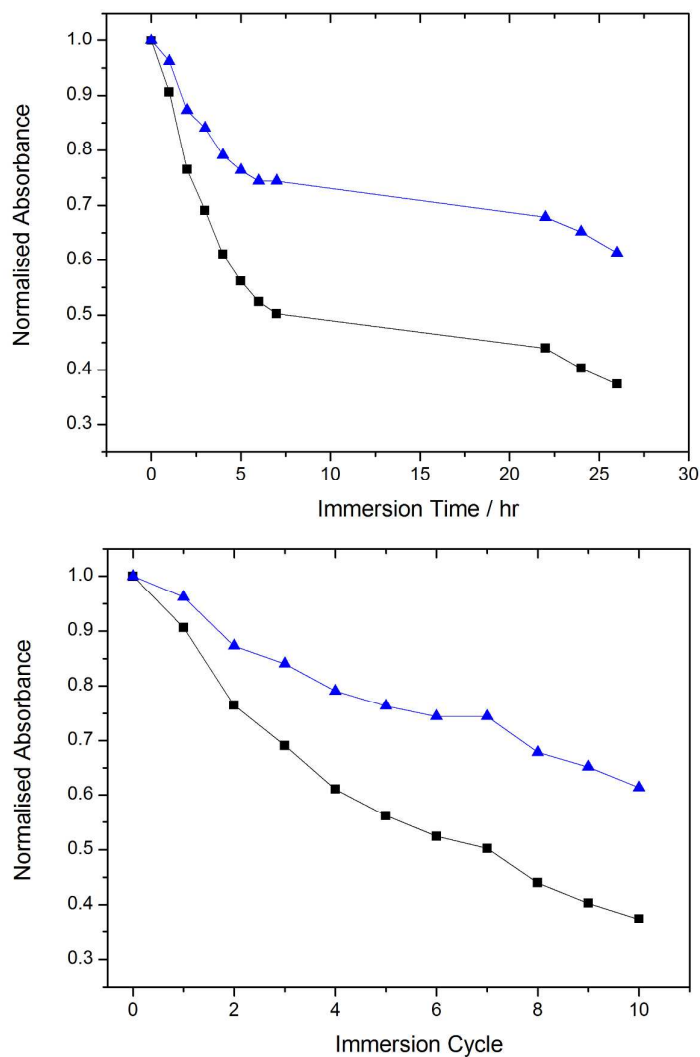
Figure 6: Top – unloading of curcumin versus immersion time from UV visible spectroscopy data, including a long timescale immersion in the middle of the dataset (filled triangles – 0.001M NaCl release solution; filled squares – 1M NaCl release solution). Bottom – the same data plotted as a function of immersion cycle number.

ATR FTIR: ATR FTIR has also been used to investigate the release kinetics of the curcumin from the polymer multilayers.   The methodology does not require the sample to be removed from solution – it is *in situ* and the PEM film is never dried at any time during the measurement.   ATR FTIR experiments were performed for multilayers loaded with curcumin, and then exposed to solutions of 1M NaCl and 0.001M NaCl.   The loading time and loading solution were identical to those used for the UV Vis experiments (12 hours; 0.001% curcumin solution in 90:10 water:ethanol).   Spectra were obtained for the loaded PEM (immediately after exposure to the salt solution for release) and for the PEM film exposed to unloading solution (1 M NaCl and 0.001 M NaCl) for 5 hours – the period during which a significant amount of release was observed in the UV Vis spectra (and normalized absorbance data shown in Figure 5).   The two pairs of spectra (loaded and following 5 hours of release) are given in Figure 7, for 0.001 M NaCl release solution and for 1 M NaCl release solution.

The major curcumin peaks are indicated by the dotted lines in the two plots.   The intensity of these two peaks can be seen to be invariant to the flowing of the release solution.   In neither 0.001 M NaCl nor 1 M NaCl is there any sign of curcumin release from the multilayers.   This observation supports the interpretation of the UV Vis release data.   For this hydrophobic molecule, embedded within the PEM film, simple exposure time in aqueous solution does not yield any release.   In contrast, when subject to successive dehydration/rehydration cycles, curcumin can be seen to be readily released from the PEM film.
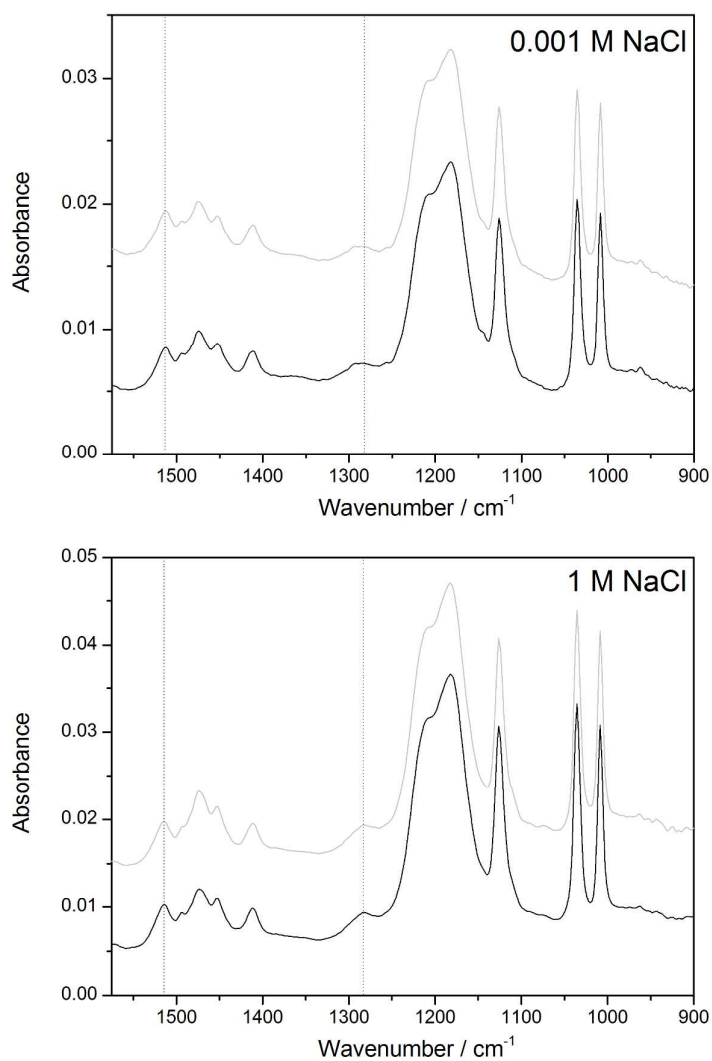
Figure 7: Spectrum of curcumin incorporated into a 5-bilayer PEM (black line) and spectrum of the same loaded multilayer exposed to NaCl release solution for 5 hours (grey line). Dotted lines indicate the positions of the two major curcumin peaks.　　Top: 0.001 M NaCl release solution.　　Bottom: 1 M NaCl release solution.

DISCUSSION

The results described above confirm previous studies of curcumin incorporation into polyelectrolyte multilayers [14], and add additional insights into the conditions required for release of the molecule upon exposure to electrolyte solutions. A key outcome is the discovery that significant release of the hydrophobic polyphenol is dependent upon the dehydration/rehydration cycle that the multilayer is subject to during the UV-Vis analysis. It is appropriate at this point to compare the release behaviour observed in the data presented above to data reported by other authors.

Guyomard et al. [2] studied the incorporation of Nile Red (a hydrophobic dye molecule) into polyelectrolyte multilayers of poly ethylene imine (PEI) and hydrophobically-modified caboxymethylpullan (CMP). Similar to the work described above, the dye molecule was incorporated for some of the work using post-PEM formation diffusion from an ethanol:water solution. Analysis of loading and release was performed using UV-Vis analysis of dry PEM films that had been exposed to varying loading and release solutions. Release was into buffer solutions of varying electrolyte composition and content (buffer or high concentration NaCl and KSCN), and varying pH.

Release was attempted into buffer solutions of close to neutral pH (which would not influence the degree of ionization of any component in the multilayer) and no dye was observed to be released from the multilayers, irrespective of the duration of immersion. The authors attributed this to the dye molecules being trapped in hydrophobic regions of the multilayer system. With buffered release solutions of lower pH (which would cause a reduction in the charge of the CMP polymer), some release was observed, but only to 30-35% of the loaded dye after 5 immersion cycles. Increased salt was seen to increase the release of the dye: with 0.5M NaCl resulting in 10% release at neutral pH (during 7 immersion cycles over almost 4 hours); and with 0.5 M KSCN resulting in nearly 50% release (during 7

immersion cycles over almost 4 hours).

Both the low/no release of dye with long timescale immersion, and the low release with 0.5M KCl (cycled immersion), is consistent with the model we propose above: release being primarily due to dehydration/rehydration cycling. No *in situ* measurement of dye release was reported in this work, and therefore it is difficult to ascertain exactly what percentage of the measured release values are due to dehydration/rehydration as opposed to diffusion. The enhanced release obtained using the KSCN electrolyte, confirms the mechanism whereby a hydrophobic dye/polyphenol could remain within a multilayer film, as KSCN was used specifically to disrupt hydrophobic interactions within the multilayer film.

More recently, Bhalerao *et al*. [43], studied the loading and release of chalcones from PSS/PDADMAC films using a similar approach of *ex-situ* UV-Vis. A maximum in absorbance of 0.14 was found for drug loading, and approximately 90% release was observed in PBS. The authors indicated potential hydrophobic interactions and π-π stacking between aromatic rings of the chalcones and PSS as intermolecular interactions that would encourage uptake into the multilayer (along with hydrogen bonding, although all proposed interactions were based on expected chemical affinities rather than any direct evidence). The same or similar interactions between drug and multilayer will be present in our example of curcumin in PDADMAC/PSS, and therefore similar retention of the chalcones within the multilayers might be expected under conditions of constant immersion, but were not observed/reported in the work of Bhalerao due to the *ex situ* nature of their analysis.

It should be noted that the mechanism postulated for our studies on curcumin (and, by extension, to the work of Guyomard et al., Bhalerao et al., and other studies of release of hydrophobic actives from PEMs) will not apply to charged dye release from PEMs (e.g. such as that described by Ball [44] and others [45, 46]) .

The second key outcome from the work reported here is the ionic strength dependence of the

dehydration/rehydration release mechanism; higher ionic strength of the release solution resulted in greater release during the multilayer rehydration. PEM characterisation studies have demonstrated that PEM layers swell and smooth with increasing ionic strength, which has been interpreted as being due to increasing water content of the layers [26]. Dodoo, et al.,[47] also proposed this increased water swelling with increasing ionic strength for PSS/PDADMAC films. It would thus be expected that rehydration of a dried multilayer would reach different levels of hydration/swelling dependent on the ionic strength of the rehydrating solution. This 'flushing' of the multilayer (which will be greater with increasing ionic strength) could explain the observed release data shown in Figures 5 and 6.

In addition to the greater influx of hydration water with higher ionic strength, the actual ion concentration from the electrolyte may contribute to the release/flushing by altering the ion-pairing (and thus multilayer permeability) between the PSS and PDADMAC. In a study of polyelectrolyte complexes between PDADMA and PSS [48], it was proposed that ions from the electrolyte specifically associated with the polymer charges in the multilayer, leading to a weakening in the polyelectrolyte ion-pairing with increasing salt content of the electrolyte [48]. However, this second potential mechanism would be expected to be just as active in a constantly immersed polyelectrolyte multilayer (which in the work reported here, does not result in drug release). Altering the ion-pairing within a multilayer through increased salt is not enough to dislodge curcumin from the film, although it may assist the removal during rehydration of the multilayer.

CONCLUSION

The loading of curcumin, a naturally-derived therapeutic hydrophobic polyphenol, into polyelectrolyte multilayers of PDADMAC and PSS has been confirmed using two spectroscopic techniques and one gravimetric technique.   The curcumin was observed to be retained in the multilayer under conditions of constant immersion in release electrolyte solution, but was seen to be released to a significant extent when the multilayers were subject to dehydration/rehydration cycles.   The release upon rehydration was found to be ionic strength dependent, and this fact is explained by the expected alteration in hydration water content and degree of ion-pairing within the multilayer when it is rehydrated with solutions of varying salt concentration.   The results highlight the need for both *in situ* and *ex situ* techniques to be used in parallel for studies of drug/bioactive molecule release, especially for hydrophobic molecules.

REFERENCES

1.   A. N. Zelikin, *ACS Nano*, 2010, 4, 2494-2509.
2.   A. Guyomard, B. Nysten, G. Müller and K. Glinel, *Langmuir*, 2006, 22, 2281-2287.
3.   M. R. Prausnitz and R. Langer, *Nat. Biotechnol.*, 2008, 26, 1261-1268.
4.   T. T. T. Nguyen, C. Ghosh, S. G. Hwang, L. D. Tran and J. S. Park, *J. Mater. Sci.*, 2013, 48, 7125-7133.
5.   M. A. Trojer, H. Andersson, Y. Li, J. Borg, K. Holmberg, M. Nyden and L. Nordstierna, *Phys. Chem. Chem. Phys.*, 2013, 15, 6456-6466.
6.   D. J. McClements, E. A. Decker and J. Weiss, *J. Food Sci.*, 2007, 72, R109-R124.
7.   L. Zhou, M. Chen, L. Tian, Y. Guan and Y. Zhang, *ACS Appl. Mater. Interfaces*, 2013, 5, 3541-3548.
8.   A. Goel, A. B. Kunnumakkara and B. B. Aggarwal, *Biochem. Pharmacol.*, 2008, 75, 787-809.
9.   R. K. Maheshwari, A. K. Singh, J. Gaddipati and R. C. Srimal, *Life Sci.*, 2006, 78, 2081-2087.
10.   M. M. Yallapu, M. Jaggi and S. C. Chauhan, *Curr. Pharm. Design*, 2013, 19, 1994-2010.
11.   S. Ganta and M. Amiji, *Mol. Pharm.*, 2009, 6, 928-939.
12.   L. Li, F. S. Braiteh and R. Kurzrock, *Cancer*, 2005, 104, 1322-1331.
13.   S. Bisht, G. Feldmann, S. Soni, R. Ravi, C. Karikar, A. Maitra and A. Maitra, *J. Nanobiotech.*, 2007, 5, 3.
14.   P. Kittitheeranun, N. Sanchavanakit, W. Sajomsang and S. T. Dubas, *Langmuir*, 2010, 10, 6869-6873.
15.   T. A. Kolesnikova, A. G. Skirtach and H. Mohwald, *Expert Opin. Drug Deliv.*, 10, 47-58.
16.   C. M. Jewell and D. M. Lynn, *Adv. Drug Deliv. Rev.*, 2008, 60, 979-999.
17.   J. A. Lichter, K. J. Van Vliet and M. F. Rubner, *Macromolecules*, 2009, 42, 8573-8586.
18.   P. K. Deshmukh, K. P. Ramani, S. S. Singh, A. R. Tekade, V. K. Chatap, G. B. Patil and S. B. Bari, *J. Control. Release*, 166, 294-306.
19.   J. B. Schlenoff, *Langmuir*, 2009, 25, 14007-14010.
20.   R. K. Subedi, S. Y. Oh, M. K. Chun and H. K. Choi, *Arch. Pharm. Res.*, 2010, 33, 339-351.
21.   A. Mukerjee and J. K. Vishwanatha, *Anticancer Res.*, 2009, 29, 3867-3875.
22.   Y. Chen, G. Zeng, F. Pan, J. Wang and L. Chi, *Langmuir*, 2013, 29, 2708-2712.
23.   Y. Jang, B. Akgun, H. Kim, S. Satija and K. Char, *Macromolecules*, 2012, 45, 3542-3549.
24.   W. Ouyang, M. Müller, D. Appelhans and B. Voit, *ACS Appl. Mater. Interfaces*, 2009, 1, 2878-2885.
25.   B. Torger and M. Müller, *Spectrochim. Acta A*, 2013, 104, 546-553.
26.   S. T. Dubas and J. B. Schlenoff, *Langmuir*, 2001, 17, 7725-7727.
27.   G. B. Sukhorukov, J. Schmidt and G. Decher, *Berichte der Bunsengesellschaft fur Physikalische Chemie*, 1996, 100, 948-953.
28.   J. Irigoyen, L. Han, I. Llarena, Z. Mao, C. Gao and S. Moya, *Macromol. Rapid Commun.*, 2012, 33, 1964-1969.
29.   F. Höök, M. Rodahl, P. Brzezinski and B. Kasemo, *Langmuir*, 1998, 14, 729-734.
30.   G. Sauerbrey, *Zeitschrift für Physik A Hadrons and Nuclei*, 1959, 155, 206-222.
31.   M. V. Voinova, M. Rodahl, M. Jonson and B. Kasemo, *Physica Scripta*, 1999, 59, 391.
32.   M. H. Rogers and G. N. Lance, *Journal of Fluid Mechanics*, 1960, 7, 617-631.

33. P. J. Sides, J. Newman, J. D. Hoggard and D. C. Prieve, *Langmuir*, 2006, 22, 9765-9769.
34. P. J. Scales, F. Grieser, T. W. Healy, L. R. White and D. Y. C. Chan, *Langmuir*, 1992, 8, 965-974.
35. I. G. Sedeva, R. Fetzer, D. Fornasiero, J. Ralston and D. A. Beattie, *J. Colloid Interface Sci.*, 2010, 345, 417-426.
36. I. G. Sedeva, D. Fornasiero, J. Ralston and D. A. Beattie, *Langmuir*, 2010, 26, 15865-15874.
37. N. Ladhari, J. Hemmerlé, Y. Haikel, J.-C. Voegel, P. Schaaf and V. Ball, *Appl. Surf. Sci.*, 2008, 255, 1988-1995.
38. D. Lin-Vien, N. B. Colthup, W. G. Fateley and J. G. Grasselli, *The Handbook of infrared and raman characteristic frequencies of organic molecules*, Academic Press, Boston, 1991.
39. S. B. Black, Y. Chang, C. Bae and M. A. Hickner, *J. Phys. Chem. B*, 2013, 117, 16266-16274.
40. S. J. Kim, S. G. Yoon, I. Y. Kim and S. I. Kim, *J. Appl. Pol. Chem.*, 2004, 91, 2876-2880.
41. M. Koperska, T. Lojewski and J. Lojewska, *Anal. Bioanal. Chem.*, 2011, 399, 3271-3283.
42. S. Detoni and D. Hadzi, *Spectrochim. Acta*, 1956, 11, 601-608.
43. U. M. Bhalerao, J. Acharya, A. K. Halve and M. P. Kaushik, *RSC Advances*, 2014, 4, 4970-4977.
44. V. Ball, *Materials*, 2012, 5, 2681-2704.
45. C. A. Ghiorghiţă, F. Bucatariu and E. S. Drăgan, *Cellul. Chem. Technol.*, 2014, 48, 247-253.
46. A. C. Pinheiro, A. I. Bourbon, M. A. C. Quintas, M. A. Coimbra and A. A. Vicente, *Innovative Food Science and Emerging Technologies*, 2012, 16, 227-232.
47. S. Dodoo, R. Steitz, A. Laschewsky and R. von Klitzing, *Phys. Chem. Chem. Phys.*, 2011, 13, 10318-10325.
48. J. A. Jaber and J. B. Schlenoff, *J. Amer. Chem. Soc.*, 2006, 128, 2940-2947.